Received: 21 August 2017 | Revised: 20 March 2018 | Accepted: 8 April 2018

DOI: 10.1002/rra.3296

RESEARCH ARTICLE

WILEY

Hydrologic scaling for hydrogeomorphic floodplain mapping: Insights into human-induced floodplain disconnectivity

Fernando Nardi[1] | Ryan R. Morrison[2] | Antonio Annis[1,3] | Theodore E. Grantham[4]

[1] Water Resource Research and Documentation Center (WARREDOC), Università per Stranieri di Perugia, Perugia, Italy

[2] Department of Civil and Environmental Engineering, Colorado State University, Fort Collins, Colorado

[3] DICEA, University of Florence, Florence, Italy

[4] Department of Environmental Science, Policy, and Management, University of California, Berkeley, Berkeley, California

Correspondence
F. Nardi, Water Resource Research and Documentation Center (WARREDOC), Università per Stranieri di Perugia, Piazza Fortebraccio, 4 06100 Perugia, Italy.
Email: fernando.nardi@unistrapg.it

Abstract

Hydrogeomorphic approaches for floodplain modelling are valuable tools for water resource and flood hazard management and mapping, especially as the global availability and accuracy of terrain data increases. Digital terrain models implicitly contain information about floodplain landscape morphology that was produced by hydrologic processes over long time periods, as well as recent anthropogenic modifications to floodplain features and processes. The increased availability of terrain data and distributed hydrologic datasets provide an opportunity to develop hydrogeomorphic floodplain delineation models that can quickly be applied at large spatial scales. This research investigates the performance of a hydrogeomorphic floodplain model in two large urbanized and gauged river basins in the United States, the Susquehanna and the Wabash basins. The models were calibrated by a hydrologic data scaling technique, implemented through regression analyses of USGS peak flow data to estimate floodplain flow levels across multiple spatial scales. Floodplain model performance was assessed through comparison with 100-year Federal Emergency Management Agency flood hazard maps. Results show that the hydrogeomorphic floodplain maps are generally consistent with standard flood maps, even when significantly and systematically varying scaling parameters within physically feasible ranges, with major differences that are likely due to infrastructure (levees, bridges, etc.) in highly urbanized areas and other locations where the geomorphic signature of fluvial processes has been altered. This study demonstrates the value of geomorphic information for large-scale floodplain mapping and the potential use of hydrogeomorphic models for evaluating human-made impacts to floodplain ecosystems and patterns of disconnectivity in urbanized catchments.

KEYWORDS

DTM, floodplain, hydrogeomorphic model, hydrologic scaling, regression analysis, USGS

1 | INTRODUCTION

Floodplains are important landscape features that provide numerous environmental and human services, including riparian habitat, pollutant removal, energy recycling, flood attenuation, and groundwater recharge. Floodplains have also been significantly modified over time by human land and water-use activities, leading to floodplain habitat loss and necessitating management of flood risks in developed areas (Nardi, Annis & Biscarini, 2018). These dual challenges of floodplain management—maintaining ecosystem benefits while protecting human development—require that floodplain areas be properly defined and delineated, especially in regions facing other water management challenges, including population growth, declining water supplies, and water quality degradation (Burt, Matchett, Goulding, Webster, & Haycock, 1999; Ignacio, Cruz, Nardi, & Henry, 2015). Floodplain maps are currently available for major rivers and cities worldwide (e.g., Di

Baldassarre, Montanari et al., 2010b; Pappenberger, Dutra, Wetterhall, & Cloke, 2013; Sampson et al., 2015; Winsemius et al., 2016), but coverage is limited in tributary and minor river networks, where the paucity of flow-measurement stations make estimating floodplain extent highly uncertain when using event-based hydrodynamic modelling approaches (Di Baldassarre, Schumann et al., 2010a), particularly at large scales (Ward et al., 2015).

Fortunately, an increasing global availability of high-accuracy Digital Terrain Models (DTMs) derived from earth observation technology (e.g., satellite, aerial, or drones) offers new opportunities for advancing large-scale floodplain mapping. DTMs have been used to implement simplified hydraulic models for river-basin scale flood mapping (Merwade, Cook, & Coonrod, 2008; Noman, Nelson, & Zundel, 2001) and to perform floodplain mapping using morphometric analysis. The latter methodology, commonly known as a geomorphic method (Gallant and Dowling (2003), McGlynn and Seibert (2003), and Dodov and Foufoula-Georgiou (2006)), aims to identify floodplains as unique morphologic landscape features within fluvial corridors that are created by erosion and depositional processes and are clearly recognizable using terrain data analyses. More recently, this floodplain delineation method has been the subject of significant interest with further investigations incorporating hydrologic (Nobre et al., 2011), geomorphic (Manfreda et al., 2014; Manfreda, Sole, & Fiorentino, 2008; Samela, Troy, & Manfreda, 2017), and soil classifications (Sangwan & Merwade, 2015) to perform large-scale floodplain mapping. Specifically, geomorphic methods use gridded watershed information related to hydrologic, geomorphic, and soil classification parameters to distinguish the floodplain domain from surrounding hillslopes. For example, Manfreda et al. (2014) used the topographic wetness index, Nobre et al. (2011) the elevational difference between channel cells and surrounding topography, and Sangwan and Merwade (2015) soil map unit (United Stated SSURGO database) parameters to delineate floodplains.

Hydrogeomorphic analyses combine hydrologic and geomorphic methods. In particular, a simplified hydrologic analysis for determining flood stage is implemented to identify gridded thresholds of floodplain terrain elevations. The floodplain zone is identified by filtering fluvial valley cells that underlay the maximum flood flow level for a specific recurrence interval. Channel flood levels are then used in equations that relate the channel flow depth to the drainage area. For example, geomorphologists have observed and measured the hydraulic geometry of stream channels using power laws, where the flow height (*FH*) is expressed as a function of the contributing area (C_A) using an exponential function (Leopold & Maddock, 1953).

Despite a growing popularity of hydrogeomorphic methods for floodplain mapping, the application of these models presents numerous difficulties. First, the lack of validation data, particularly for low-frequency flood events, is particularly challenging. Second, because hydrogeomorphic methods assume that the landscape configuration is the product of natural erosional and deposition processes operating over large time scales, the effects of recent anthropogenic modifications to floodplain features and processes can introduce substantial uncertainty in floodplain maps. The resolution and accuracy of DTMs and issues related to terrain analysis and data processing are also challenges. Finally, hydrogeomorphic methods require empirical data on flood stage to parameterize the floodplain flow depth scaling relationship, and the quality and availability of these data are expected to have a significant influence on model performance and uncertainty.

Here, we adopt Leopold and Maddock's (1953) power law and extend its application to floodplain flow depths, as tested by Bhowmik (1984), specifying the contributing area as a scaling parameter. The presented approach expands on the hydrogeomorphic floodplain model developed by Nardi et al. (2006, 2013) that was built on the principles of hydraulic geometry (Bhowmik, 1984) and fractal river basins (Tarboton, Bras, & Rodriguez-Iturbe, 1988), enforcing the theoretical principle of interlinked climatic, hydrologic, and geomorphic processes (Rodrıguez-Iturbe & Rinaldo, 1997; Vivoni, Di Benedetto, Grimaldi, & Eltahir, 2008) that govern landscape evolution (Grimaldi, Teles, & Bras, 2004; Grimaldi, Teles, & Bras, 2005; Istanbulluoglu & Bras, 2005). We implement a novel hydrologic data-driven calibration procedure to parameterize the scaling relationship of floodplain flow levels and contributing area. Distributed hydrologic data are gathered from US Geological Survey (USGS) stream gauges and statistically processed using regression analyses to estimate various recurrence interval flood stages and scaling parameters. The approach is tested in two large urbanized and gauged river basins of the United States. Standard flood hazard maps are used for evaluating floodplain delineation results. By evaluating the sensitivity of the hydrogeomorphic floodplain model to varying hydrologic scaling parameters, this work may be useful in identifying large-scale fluvial corridors in basins where hydrologic data are limited or unavailable. Model results may also offer insights into anthropogenic impacts to fluvial corridors, including floodplain disconnectivity and alteration of ecological floodplain functions.

2 | METHODOLOGY

The proposed floodplain delineation model is adapted from algorithms developed by Nardi et al. (2006, 2013) and involves the following steps:

a. DTM is processed using pit filling, flow direction estimation, and cell accumulation algorithms for each watershed cell (Jenson and Domingue, 1988; Nardi, Grimaldi, Santini, Petroselli, & Ubertini, 2008; Grimaldi, Petroselli, Alonso, & Nardi, 2010). The river network is then identified by filtering cells with a contributing area greater than a predefined threshold (Grimaldi, Nardi, Di Benedetto, Istanbullouglu, & Bras, 2007; Nardi et al., 2008; Tarboton & Ames, 2001; Tarboton, Bras, & Rodríguez-Iturbe, 1991).
b. A scaling relationship based on the work of Leopold and Maddock (1953) is applied for deriving flow heights along the river network using the upslope contributing area as scaling parameter. The scaling relationship is expressed in Equation (1):

$$FH_i = aC_A{}^b, \tag{1}$$

where FH_i is the maximum flow height (m) for the flood recurrence interval i, a, and b and are dimensionless scaling parameters, and C_A is the contributing area (m^2). In this work, scaling parameters a and b are determined by regression analyses using river flow stages for a

given recurrence interval, estimated at gauges distributed throughout the basin.

c. The floodplain is mapped using the hydrogeomorphic method approach described by Nardi et al. (2006, 2013). In general, this includes determining the maximum flood elevation using the scaling equation for *FH* (Equation (1)) and comparing the elevation to the surrounding valley bottom elevation at each stream network cell. The model results are evaluated using an objective function that quantitatively assesses overlapping regions of the floodplain with standard flood hazard maps.

Each of these steps are described in more detail in the following subsections.

2.1 | DTM processing and hydrologic data collection

The hydrogeomorphic floodplain delineation model requires data representing both the topography and hydrologic characteristics of the basin. This study used global NASA SRTM elevation data (Farr & Kobrick, 2000) to generate 30-m resolution DTMs of study basins. Flow data were obtained from USGS gauges that had at least 50 years of peak-flow records, specifically annual maximum discharge (cubic feet per second [cfs]), annual maximum stage (ft), gage baseline elevation (ft), gage datum, and longitudinal/latitude coordinates. Existing 100-year flood boundary data were collected from the Federal Emergency Management Agency (FEMA) National Flood Insurance Program. This study used data associated with "Zone AE" flood boundaries, which correspond to flood zones determined using detailed hydraulic modelling methods.

2.2 | Estimating flood stage from USGS gage data

Estimation of flood stage (at a specific recurrence-interval) at distinct locations within a study basin were generated through a semiautomated procedure for analysing USGS stream gauge data. USGS gauges within a study basin were identified and data obtained for peak annual discharge and associated stages. The peak annual data for some gauges contain inaccuracies that are noted by the USGS using qualification codes. Any observation with a qualification code indicating inaccuracies was removed. The filtered data from each gauge were used to estimate flood discharges at various return intervals if the length of record for the gauge was greater than 30 years. Regressions were fit to peak annual discharge values at each gage using the Log Pearson III distribution (United States Geological Survey (USGS), 1982) to estimate the 25-, 50- and 100-year flood discharge (Figure 1a).

To estimate the flood stage at each return-interval discharge, a local regression (LOESS) regression (Cleveland, 1979) was used to fit discharge-flood stage data at each gage. LOESS regressions fit smooth curves through scatterplots based on local, iterative, reweighted regression using nearby measurements on a point-by-point basis. Using the flood discharge values derived from the Log Pearson III distribution and the LOESS regression of stage-discharge values, the flood stage for the 25-, 50-, and 100-year recurrence interval was then estimated (Figure 1b).

2.3 | Hydrogeomorphic floodplain delineation and standard flood hazard maps

The flood stage (FH_i) estimates for all gauges within a basin were used to compute parameters *a* and *b* in Equation (1) at each recurrence interval (*i*). The fit-model was then used to predict flood height at all cells within the basin, using the contributing area of each cell (C_A). Finally, the floodplain was delineated by evaluating the elevation of each cell, along hillslope paths, as respect to the maximum flow level, FH_i. All spatially-contiguous cells underlying absolute elevation based on FH_i were mapped within the floodplain.

To evaluate the differences between the delineated hydrogeomorphic floodplain and FEMA flood boundaries derived using hydraulic modelling, an objective measure-to-fit function (*F*) was implemented (Pappenberger, Frodsham, Beven, Romanowicz, & Matgen, 2007). We assessed floodplain model results in relation to digital FEMA maps of the 100-year flood hazard zone, which are readily available for most basins in the U.S. The objective function, *F*, was calculated using Equation (2):

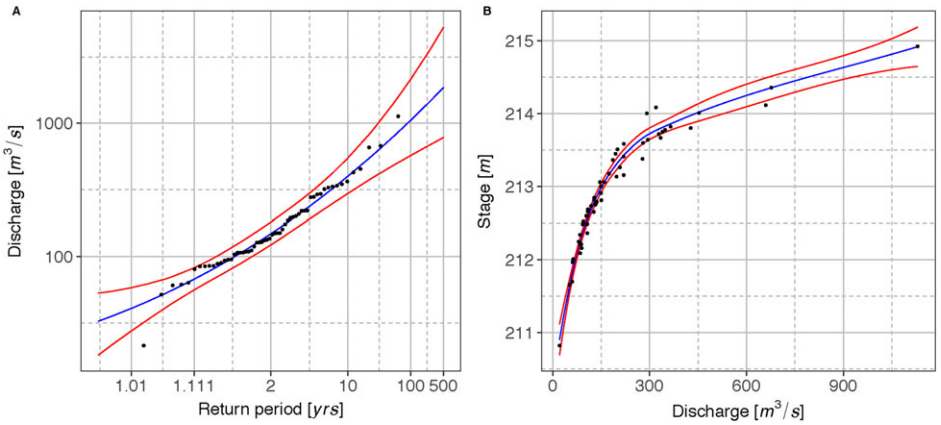

FIGURE 1 Flood frequency plot for peak discharge at US Geological Survey Gage 03340800 (left). The dots are peak annual discharge values, the solid line is the Log Pearson III distribution fit to peak discharge values, and the dashed lines are the 95% confidence intervals. LOESS regression of peak annual discharge versus stage values (right). The dots are the stage-discharge values from the gage records, the solid line is the LOESS regression curve, and the dashed lines are the 95% confidence intervals [Colour figure can be viewed at wileyonlinelibrary.com]

$$F = (A-C)/(A+B+C), \quad (2)$$

where A, B, C, and D represent overlapping, underprediction, or overprediction following the contingency scheme represented Table 1. Values of F can range between −1 (poor fit between model results and FEMA maps) to +1 (perfect fit between model results and FEMA maps).

We used Equation (2) to compare overall similarities between our model results and FEMA maps, as well as differences in model performance across Hortonian stream orders.

3 | CASE STUDY BASINS

The hydrogeomorphic floodplain model was applied to the Susquehanna and Wabash basins in the U.S. (Figure 2). These large river basins are in the Midwest and Atlantic urbanized coastal regions of the U.S., respectively, and contain abundant hydrologic datasets, including long periods of USGS gage data and FEMA 100-year flood boundaries. In addition, both basins have a history of flooding that has resulted in the construction of flood control projects, such as levees and floodwalls. A brief description of each basin is provided below.

3.1 | Susquehanna Basin

The Susquehanna Basin is approximately 71,000 km^2 and encompasses portions of New York, Pennsylvania, and Maryland states in the northeastern U.S. (Figure 2). Geologic conditions in the basin range from folded sedimentary rock in the northern and western regions of the basin to igneous and meta-volcanic rock in the southern region (Zhang, Pody, Dehoff, & Balay, 2012). Average annual precipitation varies from 84 to 199 cm depending on location in the basin and climatic interaction between Atlantic and continental air masses (Zhang et al., 2012). The Susquehanna Basin is extremely flood prone, and large flood events have occurred as recently as 2004. Dams and levees have been constructed in the basin to project against flooding, especially upstream of major cities, such as Harrisburg, Pennsylvania.

3.2 | Wabash Basin

The Wabash Basin is approximately 85,000 km^2 and encompasses parts of Indiana, Ohio, and Illinois state (Figure 2). The geology in the basin is primarily comprised of glacial till with exposed bedrock in select locations (Pyron & Neumann, 2008, United States Army Corps of Engineers (USACE), 2011). As the Wabash River approaches the Ohio River, the basin gradient decreases considerably (Pyron & Neumann, 2008). Average annual precipitation ranges between 94 and 125 cm (USACE, 2011). Large variations in discharge occur in unregulated streams within the basin, with the largest flows occurring between December and May (USACE, 2011). Frequent flooding has led to the construction of levees and floodwalls throughout the basin to protect agricultural and urban areas. The largest flood on record occurred in 1937 near the mouth of the Wabash River, but more recent floods have occurred in 2008 and 2011 (USACE, 2011).

TABLE 1 Contingency table showing F index variables from Equation (2)

	Within the FEMA map	Outside the FEMA map
Within the floodplain	A	B
Outside the floodplain	C	D

Note. FEMA: Federal Emergency Management Agency.

4 | RESULTS

4.1 | Calibrating the floodplain flow depth scaling law parameters

Scaling parameters were estimated using regression analyses of USGS peak annual discharge and stage data from 14 gauges in the Susquehanna Basin and 17 gauges in the Wabash Basin (Table 2). The average lengths of record for gauges selected in the Susquehanna and Wabash Basins were 91 and 83 years, respectively. Gauges were selected that represented a range of geographic locations and stream orders within each basin (Figure 2). Flow depths (FH_i) for the 25-, 50-, and 100-year flood frequencies (determined using flood frequency analysis and LOESS regressions previously described) and upstream contributing areas (C_A) at each gage were used to estimate the a and b scaling parameters. Figure 3 shows the regression plots for the 100-year flood for the Susquehanna and Wabash basins and the corresponding fitting of statistically inferred data from observations of the Leopold's power law (R^2 = 0.89 and 0.88, respectively). Calibrated values for the scaling parameters are a = 0.0635 and b = 0.2006 for the Susquehanna basin and a = 0.0007 and b = 0.3972 for the Wabash basin.

4.2 | Floodplain mapping varying recurrence intervals and sensitivity analysis of scaling parameters

Floodplain modelling was performed using the flow depth scaling regression for hydrologic flood frequencies of 25-, 50-, and 100-year recurrence intervals. Figure 4 illustrates the results of floodplain mapping with varying recurrence intervals. Because the hydrologic processes responsible for shaping floodplain topography are associated with low frequency, high flow-volume floods (Bhowmik, 1984), the 100-year event was selected as the most appropriate return interval for more detailed analyses.

The sensitivity of hydrologic scaling on the geomorphic floodplain mapping results was tested by systematically varying the scaling parameters, a and b. A predefined range of a and b parameters was selected, pertaining to a physically feasible range (Nardi et al., 2006), and corresponding floodplain delineations were produced. An F-index was computed using the delineated floodplain for each a and b combination. A total of 55 combinations of a and b parameters were tested ranging, respectively, from 0.05 to 0.07 and 0.18 to 0.28 for the Susquehanna basin and 0.0005 to 0.001 and 0.35 to 0.45 for the Wabash basin.

The hydrogeomorphic floodplain modelling results using the USGS-calibrated scaling parameters and the varying scaling conditions were plotted and compared with the 100-year floodplain boundary in each basin. Figures 5 and 6 show basin-wide and detailed insets of the floodplain delineations for each basin, as well as the FEMA 100-year flood boundaries located in the same areas.

Differences between the hydrogeomorphic modelling results and FEMA flood hazard maps were evaluated using the objective function

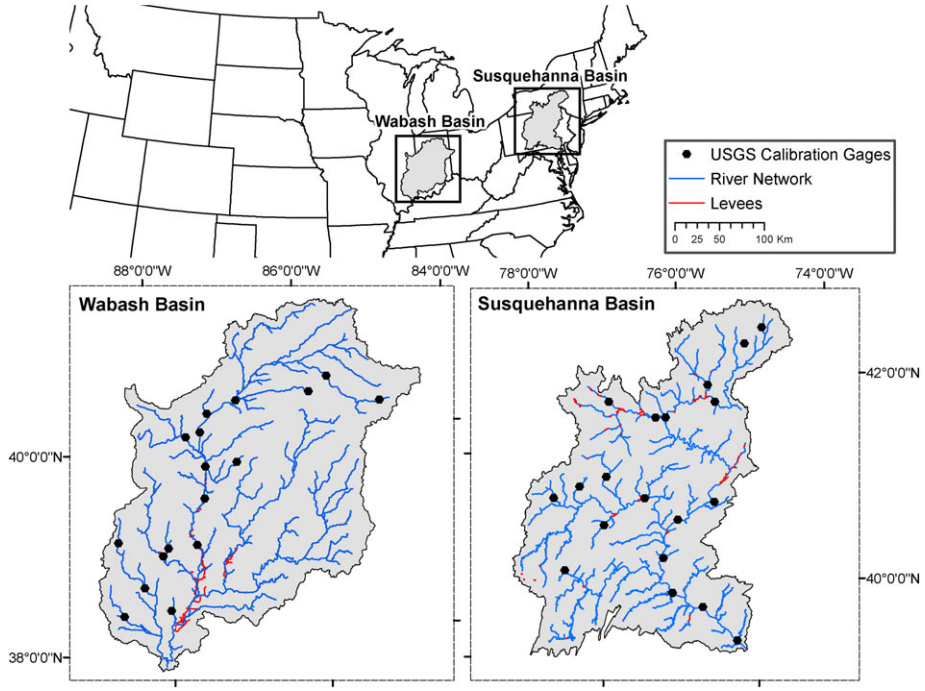

FIGURE 2 The geographic setting of the selected study basins: The Wabash and Susquehanna basins in the eastern USA with representation of the river network and US Geological Survey (USGS) gage and levee distribution [Colour figure can be viewed at wileyonlinelibrary.com]

TABLE 2 USGS gauges in each basin used for calibration. The 100-year flood stage was determined using LOESS regressions of peak annual flood discharges and stage

Susquehanna Basin				Wabash Basin			
USGS Gage Number	C_A, km^2	Elevation, m.a.s.l.	100-year stage, m.a.s.l.	USGS Gage Number	C_A, km^2	Elevation, m.a.s.l.	100-year stage, m.a.s.l.
01502000	150.0	335	336.90	03333450	117.4	254	254.84
01496500	269.4	358	360.3	03378000	344.6	119	121.3
01555500	411.8	125	129.3	03325500	366.9	297	298.7
01543000	772.3	273	277.0	03340800	420.0	214	214.8
01547500	876.7	177	180.2	03378635	616.7	158	159.9
01529500	1227.4	309	313.1	03335700	827.4	159	160.5
01548500	1545.1	238	242.5	03346000	862.4	145	146.6
01503000	5785.0	257	263.8	03380500	1087.5	120	124.3
01531000	6499.3	238	245.0	03326500	2343.2	238	N/A
01515000	12324.5	228	234.7	03379500	2836.0	124	N/A
01551500	14692.5	155	161.3	03339000	3274.9	159	162.2
01540500	28967.7	132	140.7	03345500	3810.4	137	144.2
01570500	62222.3	89	97.4	03335500	18213.1	152	162.1
01576000	66857.9	71	80.3	03336000	20576.5	144	153.89
				03340500	27969.2	140	149.5
				03341500	31000.2	134	144.7
				03342000	33263.5	124	134.8

Note. USGS: US Geological Survey.

(Equation (2)). The F-indices calculated using USGS-calibrated scaling parameters for the Susquehanna and Wabash basins were 0.24 and 0.34, respectively. Changes in F-indices due to sensitivity analyses of the scaling parameters are shown in Figure 7. Results show that the hydrogeomorphic floodplain adequately and consistently represent flood prone areas for a wide range of hydrologic scaling parameters.

4.3 | Hydrogeomorphic floodplain behaviour with varying stream orders

Figure 8 shows variations in F-index values across Hortonian stream orders. Median F-index values generally increased with stream order in each basin, ranging from approximately 0.1 in first-order streams

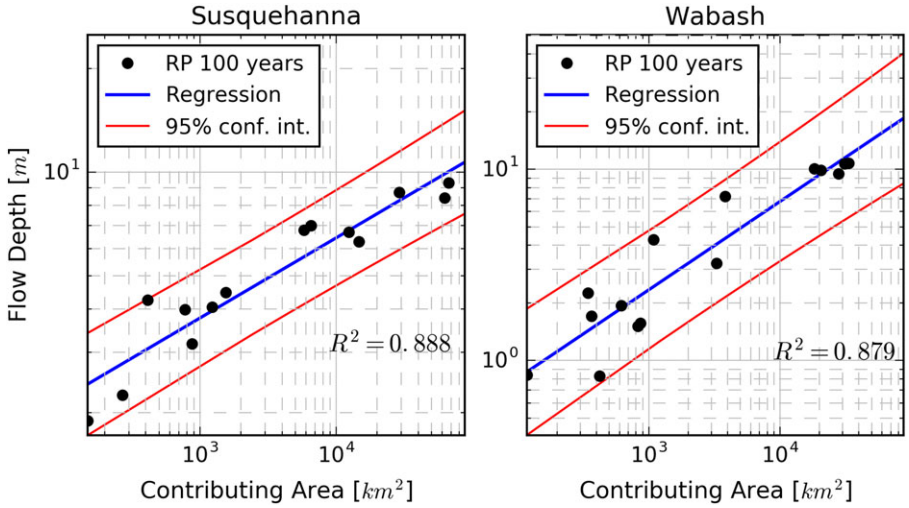

FIGURE 3 Regression plots used to determine the scaling parameters for the 100-year flood frequency in each basin. Each circle represents data for flood depth (*FH*) and contributing area (*A*) for single gage in a basin. The regression was used to determine the *a* and *b* scaling parameters for the scaling law $FH = aC_A^b$ [Colour figure can be viewed at wileyonlinelibrary.com]

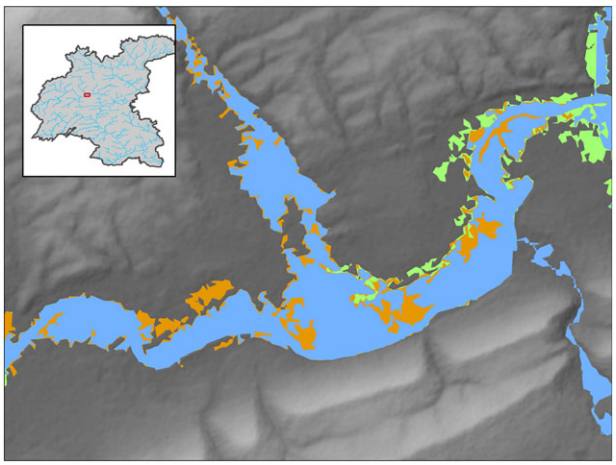

FIGURE 4 Floodplain modelling results for a sample area of the Susquehanna Basin for 25- (light blue), 50- (orange), and 100-year (green) recurrence intervals [Colour figure can be viewed at wileyonlinelibrary.com]

to 0.65 in fifth-order streams. F-index variability also tended to increase with stream order, though variability in first-order streams within the Wabash Basin was particularly high. Values associated with calibrated *a* and *b* scaling parameters were close to the median F-index values, especially in the Wabash Basin.

5 | DISCUSSION

5.1 | Model results and floodplain mapping sensitivity to hydrologic scaling

Results show that the hydrogeomorphic floodplain was generally consistent with the 100-year FEMA flood boundaries. Visual comparison of model delineations (for instance, see Inset 1 of Figure 4) and quantitative comparison analyses with Equation (2) show that the hydrogeomorphic floodplain results consistently mimic the geometry of flood hazard zones, especially in areas that contain little human-made floodplain modifications. The scaling relationships had high coefficients of determination for a 100-year flood frequency in both case study basins, indicating that the predictions of flood stage in the basins were reliable. Major differences between the modelled and FEMA-mapped floodplain boundaries are likely due to water infrastructure (levees, bridges, etc.) that directly alter flood hydraulics and disrupt connectivity between the river channel and floodplain. Quantitative comparisons of model results to FEMA flood boundaries yielded F-indices of 0.24 (Susquehanna) and 0.34 (Wabash) when using USGS data for calibrating the flow depth Leopold's scaling law. The F-index was consistently greater than 0.10 during the scaling parameter sensitivity analyses.

Assessments of model performance in this study, as well as in similar floodplain mapping research, is limited to areas where FEMA or other reference flood maps are available. Considering that field surveys for validation are only available at the local scale and that, at the large scale, floodplain maps tend to be produced in areas with high levels of human development, discrepancies between the hydrogeomorphic floodplain and hydraulic floodplain are likely to be significant. Thus, F-index values are not expected to be as high (i.e., close to a value of 1) as might be observed in more natural settings (Schumann et al., 2005). Discrepancies of the geomorphic floodplain models are not only due to the hydraulic impacts of human alterations in fluvial corridor, but also because the approach that floodplain landscapes are primarily created by large-scale hydrologic forces over extended periods of time, as opposed to localized hydraulic interactions (Nardi et al., 2006; Nardi, Biscarini, Di Francesco, Manciola, & Ubertini, 2013). This fundamental methodological aspect needs be considered when evaluating performance relative to standard flood hazard maps.

It is important to note that the discharge and river stage values that we calculated for various flood frequencies are dependent on the length of USGS gage records. At lower-frequency return periods, such as the 100-year event, relatively short lengths of hydrologic data used for flood frequency analyses can lead to reduced confidence in the results (e.g., Bhuyian, Kalyanapu, & Nardi, 2014; Kidson &

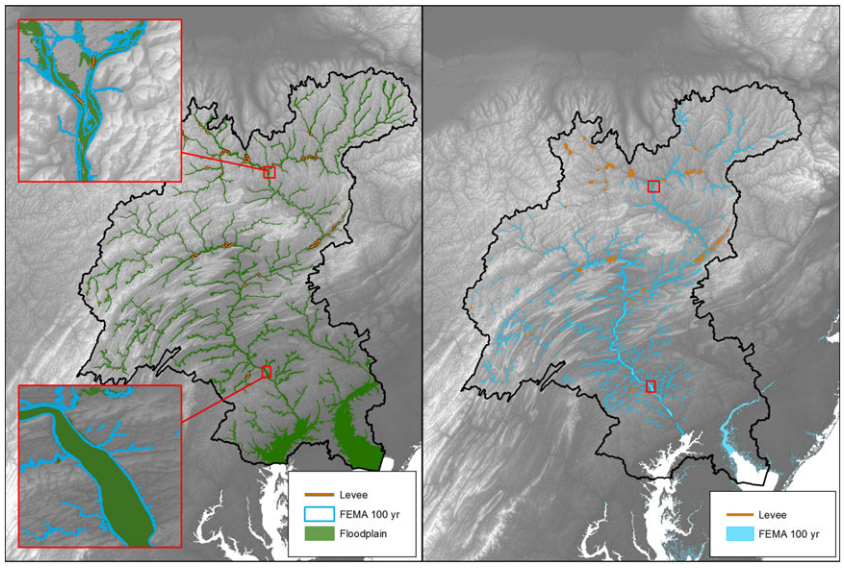

FIGURE 5 Floodplain modelling results for the Susquehanna Basin. Calibrated floodplain delineation results are shown on the left, and insets 1 and 2 depict the floodplain delineation and the Federal Emergency Management Agency (FEMA) 100-year flood boundary. The inset locations were chosen to highlight the difference between FEMA and calibrated model results when levees are present [Colour figure can be viewed at wileyonlinelibrary.com]

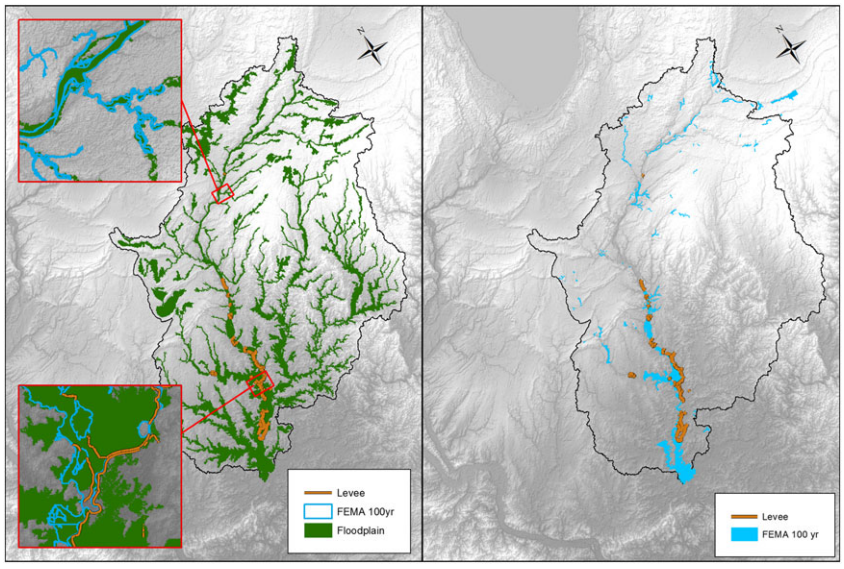

FIGURE 6 Floodplain modelling results for the Wabash basin. Calibrated floodplain delineation results are shown on the left, and insets 1 and 2 depict the floodplain delineation and the Federal Emergency Management Agency (FEMA) 100-year flood boundary. The inset locations were chosen to highlight the difference between FEMA and calibrated model results when levees are present [Colour figure can be viewed at wileyonlinelibrary.com]

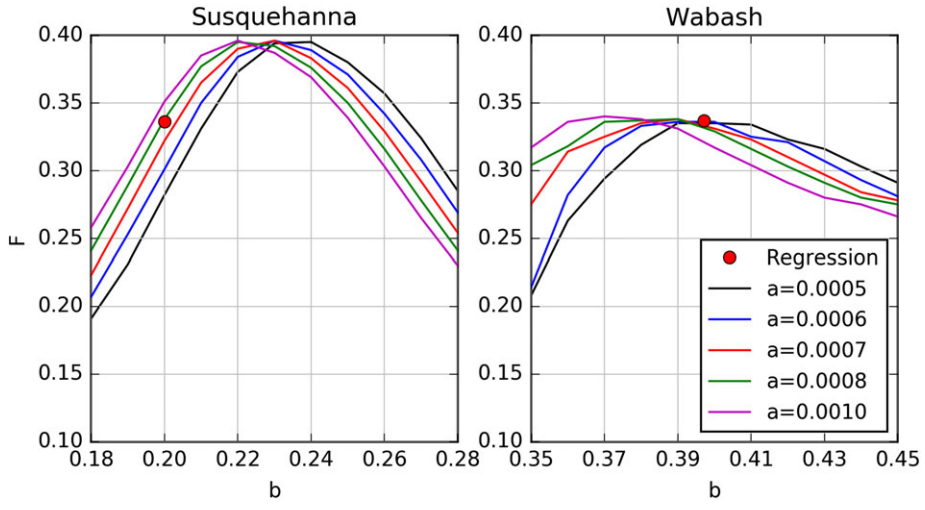

FIGURE 7 Validation analyses using the measure of fit F-index with varying combination of *a* and *b* scaling parameters for the Susquehanna and Wabash basins. The red dot shows the F-index for the calibrated *a* and *b* parameters used in the model [Colour figure can be viewed at wileyonlinelibrary.com]

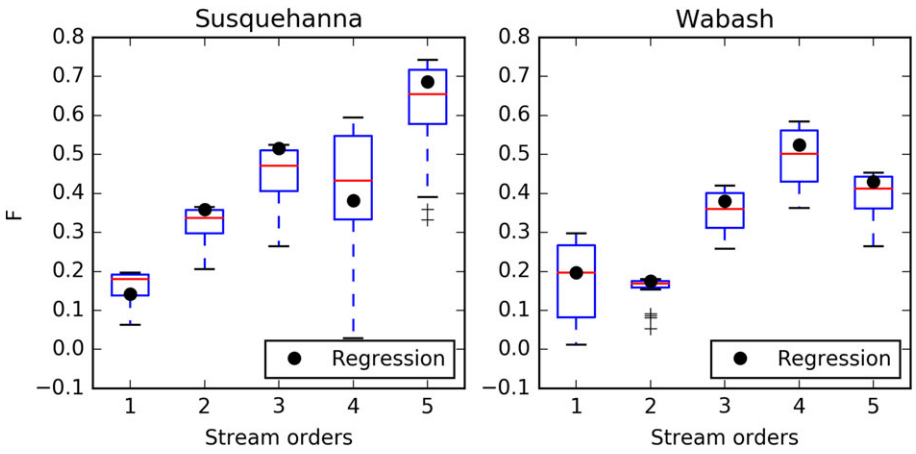

FIGURE 8 Box plots of the measure-to-fit F index representing the performance of the hydrogeomorphic floodplain model as respect to Federal Emergency Management Agency 100-year recurrence interval flood hazard maps for the Susquehanna and the Wabash basins. F indices are sampled with stream orders with varying *a* and *b* as respect to the calibrated scaling law parameters (regression) [Colour figure can be viewed at wileyonlinelibrary.com]

Richards, 2005). Flood frequencies estimated using inadequate lengths of record may contain more uncertainty in their ability to represent the discharges that drive hydrogeomorphic processes. Although there is not a consensus on the appropriate record length for determining flood frequencies, this study sought to include gauges with observation lengths of at least 30 years (after data filtering). The average post-filtered lengths of record for gauges selected in the Susquehanna and Wabash Basins were 83 and 74 years, respectively. In addition, human-induced manipulations of river discharges through water management activities have undoubtedly altered long-term discharge datasets. Although the USGS data used in this study were filtered to remove outliers, the influence of water management operations on flood frequencies and flood stage were not considered.

The sensitivity analyses (Figure 7) revealed that F-indices are most stable at an optimal value for the *b* parameter. The analyses also show that model performance can noticeably change when the *b* parameter varies from its optimal value (e.g., in the Wabash basin, ±0.05 variation in *b* from the optimal value decreases the F-index by 0.05). However, the model performance was less sensitive to changes in *a* parameter values. It is important to note that the optimal values for *a* or *b* may not be the same as the calibrated value, as illustrated in Figure 7. These sensitivity results highlight the relative importance of each parameter in the hydrogeomorphic model. For instance, the *a* parameter is defined by the minimum contributing area located at the headwaters of the stream network and therefore has little impact on floodplain delineations in stream networks lower in a basin. However, the *b* parameter can strongly influence floodplain flow depths, particularly in flat fluvial corridors that are poorly bound by sharp valley breaks. Nevertheless, it is noted that fluvial valleys are generally well-defined within DTMs with respect to surrounding sloping hills. Consequently, widely varying *b* parameters can result in consistent floodplain zoning.

Results from the sensitivity analyses (Figure 7) were determined by averaging the model performance at the basin scale. However, it important to evaluate the performance of the model within diverse hydrologic and geomorphic conditions that characterize the basin across the multiple spatial scales. Therefore, we partitioned the sensitivity results according to Hortonian stream order to investigate the spatially distributed impact of scaling law parameters on the floodplain model results. We expected archetype longitudinal geomorphic characteristics of river networks to influence the results in Figure 8. For instance, headwater river corridors tend to be more confined compared with wider downstream valleys, which often contain terraced hillslopes and other complexities. Therefore, it is not surprising that F-index values associated with lower order streams (e.g., first- and second-order streams) generally contained less variability compared with higher-order streams, since topographic variability in downstream river corridors tends to increase as well. However, because downstream river corridors are often more discernable in coarser DTM resolution, such as the 30-m DTM resolution used in this study, the model was more successful at identifying floodplains in higher-order segments, creating greater F-index values. We found these fluvial geomorphic controls were well reflected in the results for the Susquehanna basin (Figure 8). The results for the Wabash basin, however, were more varied, likely because of significant human development in floodplains, such as levees and embankment construction (e.g., consider the number of levees shown in Figure 6 compared with Figure 5). Further investigations on the spatial distribution of the performance analyses is out of the scope of this work but worth considering in future research but suggest that human modifications to floodplains can strongly influence floodplain identification.

5.2 | Human impacts and floodplain hydro-ecologic disconnectivity

The goal of this study was not to evaluate the performance of the hydrogeomorphic model as a potential substitute of standard advanced flood models but rather to evaluate the validity of the proposed theoretical framework for defining fluvial corridors as geomorphic evidences of hydrologic processes. Modifications to floodplain topography, such as the construction of levees, bridge embankments, or other additional flow channels, are likely to hydraulically alter floodplain boundaries (usually by restricting the available area for flooding) such that they no longer align with naturally formed fluvial corridors.

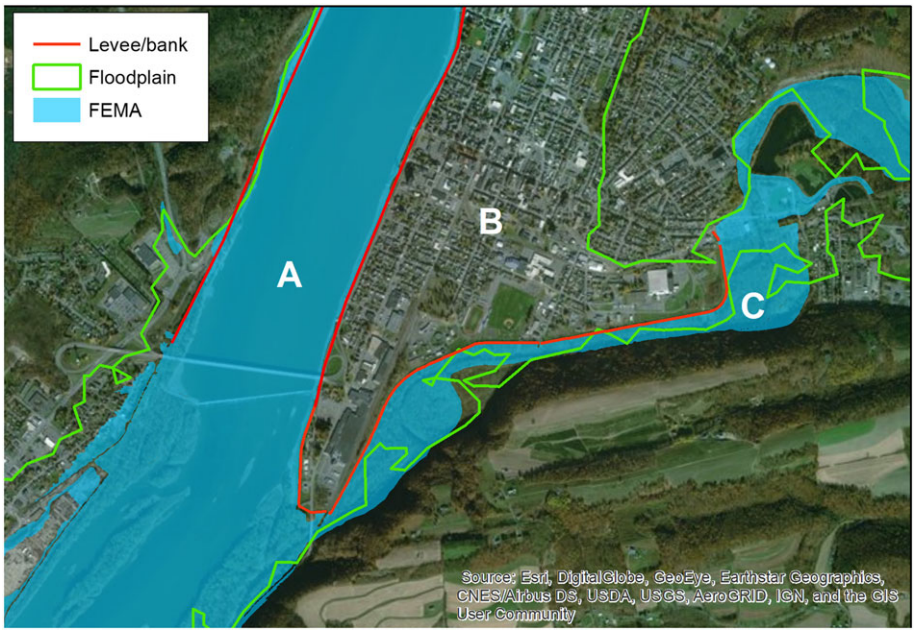

FIGURE 9 Representation of the disconnectivity of the floodplain in presence of levees with sample results of the floodplain and the different zones (A, B, and C) corresponding to the contingency table of the F index and a schematic of floodplain cross section is shown below conceptualizing the comparative analysis of the hydrogeomorphic approach (with varying FH scaling law) as respect to the 100-year Federal Emergency Management Agency (FEMA) flood hazard map [Colour figure can be viewed at wileyonlinelibrary.com]

Therefore, it is expected that model results for urbanized basins in the presence of flood control infrastructure, would be characterized by lower F-indices. F-index results illustrate the potential to use this measure-to-fit index or similar objective function to quantitatively evaluate the spatial correlation between the floodplain width and human alterations paving the way to large-scale analyses of floodplain disconnectivity due to anthropogenic territorial transformations across multiple temporal and spatial scales. Thus, we suggest the use of the F-index as a potential surrogate for quantitative analyses for evaluating portions of floodplains that are disconnected by levees and other human-built features. This is illustrated in Figures 8 that shows the diverse performance of the floodplain model at various river network positions. Landscape modifications, particularly in downstream regions of a basin, have the potential to limit floodplain variability (e.g., Figure 8) within a river network, especially in urbanized regions that contain levees or embankments. A schematic representation of an urbanized floodplain model is shown in Figure 9 (B zones are generally representing the disconnected floodplain zones).

Thus, the proposed method may identify portions of the "natural" hydrogeomorphic floodplain that are impacted by human development with significant implications for aquatic ecosystems (Di Baldassarre et al., 2017) and ecosystem services (e.g., Opperman, Luster, McKenney, Roberts, & Meadows, 2010; Stone, Byrne, & Morrison, 2017). Given the ecological importance of floodplains, understanding the spatial extent of floodplains, and the degree to which they have been altered is of significant concern to natural resource managers. The hydrogeomorphic floodplain model may particularly useful for rapidly mapping floodplains in regions, where resources for hydraulic-based methods are not available as well as for assessing the condition of fluvial corridors and to evaluate the relative degree to which floodplain connectivity has been disrupted.

6 | CONCLUSIONS

This research investigates a hydrogeomorphic method for delineating floodplain boundaries and its applications for understanding the human impact on floodplain disconnectivity in urbanized basins. The proposed large-scale floodplain model can capture the geomorphic signature of fluvial corridors using a DTM-based approach when calibrated with hydrologic data at stream gauge locations. The hydrogeomorphic model was applied in two large U.S. basins and results were compared with FEMA flood hazard maps using an objective function. The purpose of the comparative analyses was to understand differences of the two floodplain modelling approaches and the potential value of hydrogeomorphic floodplain information, rather than to advocate for the replacement of hydraulic modelling approaches for delineating floodplains. Differences in flood boundaries between the hydrogeomorphic floodplain and hydraulic mapping results reflect model uncertainty and the different theoretical paradigm of the presented hydrogeomorphic model, but are also indicative of the effects of human modifications to the fluvial corridor. The approach can be applied in other basins for quickly mapping floodplain areas over large spatial scales. The simple scaling law used in the model allows it to be generalizable across any basin and can be calibrated with hydrologic data or applied to ungauged basins for first-order estimates of floodplain extent. Further research is underway to use the hydrogeomorphic model as a tool to quantitatively evaluate the hydro-ecologic implications of large scale human-made transformations of fluvial corridors.

ACKNOWLEDGEMENTS

We would like to thank the editor and the two anonymous reviewers that helped us improve the quality of this manuscript. Fernando Nardi

and Antonio Annis gratefully acknowledge the support of the Water Resource Research and Documentation Center of University for Foreigners of Perugia and fundings from Regione Lazio Grant A11598 (Research grant "Media Valle del fiume Tevere"). Ryan Morrison and Ted Grantham were partially supported by funds from the U.S. Geological Survey Fort Collins Science Center.

ORCID

Fernando Nardi http://orcid.org/0000-0002-6562-3159
Ryan R. Morrison http://orcid.org/0000-0002-8612-1684
Antonio Annis http://orcid.org/0000-0001-6162-4691

REFERENCES

Bhowmik, N. G. (1984). Hydraulic geometry of floodplains. *Journal of Hydrology*, *68*, 369–374.

Burt, T. P., Matchett, L. S., Goulding, K. W. T., Webster, C. P., & Haycock, N. E. (1999). Denitrification in riparian buffer zones: The role of floodplain hydrology. *Hydrological Processes*, *13*(10), 1451–1463.

Bhuyian, M. N., Kalyanapu, A. J., & Nardi, F. (2014). Approach to digital elevation model correction by improving channel conveyance. *Journal of Hydrologic Engineering*, *20*(5). 04014062

Cleveland, W. S. (1979). Robust locally-weighted regression and smoothing scatterplots. *Journal of the American Statistical Association*, *74*, 829–836.

Di Baldassarre, G., Schumann, G., Bates, P., Freer, J., & Beven, K. (2010a). Floodplain mapping: A critical discussion on deterministic and probabilistic approaches. *Hydrological Sciences Journal*, *55*(3), 364–376.

Di Baldassarre, G., Montanari, A., Lins, H., Koutsoyiannis, D., Brandimarte, L., & Blöschl, G. (2010b). Flood fatalities in Africa: From diagnosis to mitigation. *Geophysical Research Letters*, *37*(22), L22402.

Di Baldassarre, G., Saccà, S., Aronica, G. T., Grimaldi, S., Ciullo, A., & Crisci, M. (2017). Human-flood interactions in Rome over the past 150 years. *Advances in Geosciences*, *44*, 9–13.

Dodov, B. A., & Foufoula-Georgiou, E. (2006). Floodplain morphometry extraction from a high-resolution digital elevation model: A simple algorithm for regional analysis studies. *IEEE Transactions on Geoscience and Remote Sensing*, *3*(3), 410–413.

Farr, T. G., & Kobrick, M. (2000). Shuttle Radar Topography Mission produces wealth of data. *EOS Trans. AGU*, *81*(48), 583–585.

Gallant, J. C., & Dowling, T. I. (2003). A multiresolution index of valley bottom flatness for mapping depositional areas. *Water Resources Research*, *39*(12), 1347. https://doi.org/10.1029/2002WR001426

Grimaldi, S., Teles, V., & Bras, R. L. (2004). Sensitivity of a physically based method for terrain interpolation to initial conditions and its conditioning on stream location. *Earth Surface Processes and Landforms*, *29*(5), 587–597.

Grimaldi, S., Teles, V., & Bras, R. L. (2005). Preserving first and second moments of the slope area relationship during the interpolation of digital elevation models. *Advances in Water Resources*, *28*, 583–588. https://doi.org/10.1016/j.advwatres.2004.11.014

Grimaldi, S., Nardi, F., Di Benedetto, F., Istanbullouglu, E., & Bras, R. L. (2007). A physically-based method for removing pits in digital elevation models. *Advances in Water Resources*, *30*(10), 2151–2158.

Grimaldi, S., Petroselli, A., Alonso, G., & Nardi, F. (2010). Flow time estimation with variable hillslope velocity in ungauged basins. *Advances in Water Resources*, *33*(10), 216–1223.

Ignacio, J. A. F., Cruz, G. T., Nardi, F., & Henry, S. (2015). Assessing the effectiveness of a social vulnerability index in predicting heterogeneity in the impacts of natural hazards: Case study of the Tropical Storm Washi flood in the Philippines. *Vienna Yearbook of Population Research*, 91–129.

Istanbulluoglu, E., & Bras, R. L. (2005). Vegetation-modulated landscape evolution: Effects of vegetation on landscape processes, drainage density, and topography. *Journal of Geophysical Research, Earth Surface*, *110*, F2.

Jenson, S. K., & Domingue, J. O. (1988). Extracting topographic structure from digital elevation models. *Photogrammetric Engineering & Remote Sensing*, *54*, 1593–1600.

Kidson, R., & Richards, K. S. (2005). Flood frequency analysis: Assumptions and alternatives. *Progress in Physical Geography*, *29*, 392–410. https://doi.org/10.1191/0309133305pp454ra

Leopold, L. B. & Maddock, T. (1953). The hydraulic geometry of stream channels and some physiographic implications, U.S Geological Survey Professional Paper, 252, 57 pp.

Manfreda, S., Sole, A., & Fiorentino, M. (2008). Can the basin morphology alone provide an insight into floodplain delineation? *WIT Transactions on Ecology and the Environment*, *118*, 47–56.

Manfreda, S., Nardi, F., Samela, C., Grimaldi, S., Taramasso, A. C., Roth, G., & Sole, A. (2014). Investigation on the use of geomorphic approaches for the delineation of flood prone areas. *Journal of Hydrology*, *517*, 863–876.

Merwade, V., Cook, A., & Coonrod, J. (2008). GIS techniques for creating river terrain models for hydrodynamic modeling and flood inundation mapping. *Environmental Modelling & Software*, *23*(10), 1300–1311.

McGlynn, B. L., & Seibert, J. (2003). Distributed assessment of contributing area and riparian buffering along stream networks. *Water Resources Research*, *39*(4), 1082. https://doi.org/10.1029/2002WR001521

Nardi, F., Vivoni, E. R., & Grimaldi, S. (2006). Investigating a floodplain scaling relation using a hydrogeomorphic delineation method. *Water Resources Research*, *42*, W09409.

Nardi, F., Grimaldi, S., Santini, M., Petroselli, A., & Ubertini, L. (2008). Hydrogeomorphic properties of simulated drainage patterns using digital elevation models: The flat area issue. *Hydrological Sciences Journal*, *53*(6), 1176–1193.

Nardi, F., Biscarini, C., Di Francesco, S., Manciola, P., & Ubertini, L. (2013). Comparing a large-scale DEM-based floodplain delineation algorithm with standard flood maps: The Tiber River Basin case study. *Irrigation and Drainage*, *62*(S2), 11–19.

Nardi, F., Annis, A., & Biscarini, C. (2018). Urbanization impact on flood hydrology within the city of Rome. J. *Flood Risk Manage*, *11*, S594–S603. https://doi.org/10.1111/jfr3.12186

Nobre, A. D., Cuartas, L. A., Hodnett, M., Rennó, C. D., Rodrigues, G., Silveira, A., … Saleska, S. (2011). Height Above the Nearest Drainage —A hydrologically relevant new terrain model. *Journal of Hydrology*, *404*(1–2), 13–29. ISSN 0022-1694, https://doi.org/10.1016/j.jhydrol.2011.03.051

Noman, N. S., Nelson, E. J., & Zundel, A. K. (2001). Review of automated floodplain delineation from digital terrain models. *Journal of Water Resources Planning and Management*, *127*(6), 394–402.

Opperman, J. J., Luster, R., McKenney, B. A., Roberts, M., & Meadows, A. W. (2010). Ecologically functional floodplains: Connectivity, flow regime, and scale. *Journal of the American Water Resources Association (JAWRA)*, *46*(2), 211–226. https://doi.org/10.1111/j.1752-1688.2010.00426.x

Pappenberger, F., Frodsham, K., Beven, K., Romanowicz, R., & Matgen, P. (2007). Fuzzy set approach to calibrating distributed flood inundation models using remote sensing observations. *Hydrology and Earth System Sciences*, *11*, 739–752.

Pappenberger, F., Dutra, E., Wetterhall, F., & Cloke, H. (2013). Deriving global flood hazard maps of fluvial floods through a physical model cascade. *Hydrology and Earth System Sciences*, *16*, 4143–4156.

Pyron, M., & Neumann, K. (2008). Hydrologic alterations in the Wabash River watershed, USA. *River Research and Applications*, *24*, 1175–1184. https://doi.org/10.1002/rra.1155

Rodrıguez-Iturbe, I., & Rinaldo, A. (1997). *Fractal river networks: Chance and self-organization*. New York: Cambridge Univ. Press.

Samela, C., Troy, T. J., & Manfreda, S. (2017). Geomorphic classifiers for flood-prone areas delineation for data-scarce environments. *Advances in Water Resources*, *102*, 13–28.

Sampson, C. C., Smith, A. M., Bates, P. D., Neal, J. C., Alfieri, L., & Freer, J. E. (2015). A high-resolution global flood hazard model. *Water Resources Research*, *51*, 7358–7381.

Sangwan, N., & Merwade, V. (2015). A faster and economical approach to floodplain mapping using soil information. *JAWRA Journal of the American Water Resources Association*, *51*, 1286–1304.

Schumann, G., J. B. Henry, L. Hoffmann, Pfister L., Pappenberger F., Matgen P. (2005). Demonstrating the high potential of remote sensing in hydraulic modelling and flood risk management. Portsmouth, U. K.: Annual Conference of the Remote Sensing and Photogrammetry Society With the NERC Earth Observation Conference, Remote Sens. and Photogramm. Soc.

Stone, M. C., Byrne, C. F., & Morrison, R. R. (2017). Evaluating the impacts of hydrologic and geomorphic alterations on floodplain connectivity. *Ecohydrology*, *2017*, e1833. https://doi.org/10.1002/eco.1833

Tarboton, D. G., Bras, R. L., & Rodríguez-Iturbe, I. (1991). On the extraction of channel networks from digital elevation data. *Hydrological Processes*, *5*(1), 81–100.

Tarboton, D. G., Bras, R. L., & Rodriguez-Iturbe, I. (1988). The fractal nature of river networks. *Water Resources Research*, *24*, 137–1322.

Tarboton, D. G.,Ames, D. P. (2001). Advances in the mapping of flow networks from digital elevation data. In: World Water and Environmental Resources Congress (Orlando, Florida, 20–24 May). Am. Soc. Civil Engrs, USA.

United States Army Corps of Engineers (USACE) (2011). Wabash River Watershed Section 729 Initial Watershed Assessment.

United States Geological Survey (USGS) (1982). U.S. Geological Survey Advisory Committee on Water Data, Guidelines for determining flood flow frequency, Bulletin 17-B of the Hydrology Subcommittee: Reston, Virginia, U.S. Geological Survey, Office of Water Data Coordination, 183 p.

Vivoni, E. R., Di Benedetto, F., Grimaldi, S., & Eltahir, E. A. B. (2008). Hypsometric control on surface and subsurface runoff. *Water Resources Research*, *44*(12), W12502.

Ward, P. J., Jongman, B., Salamon, P., Simpson, A., Bates, P., De Groeve, T., … Winsemius, H. C. (2015). Usefulness and limitations of global flood risk models. *Nature Climate Change*, *5*(8), 712–715.

Winsemius, H. C., Aerts, J. C. J. H., van Beek, L. P. H., Bierkens, M. F. P., Bouwman, A., Jongman, B., … Ward, P. J. (2016). Global drivers of future river flood risk. *Nature Climate Change*, *6*, 381–385.

Zhang, Z., Pody, R. D., Dehoff, A. D., & Balay, J. W. (2012). Analysis of streamflow trend in the Susquehanna River Basin, USA. In *Hydrologic time series analysis: Theory and practice* (pp. 181–200). New Delhi, India: Springer Netherlands.

How to cite this article: Nardi F, Morrison RR, Annis A, Grantham TE. Hydrologic scaling for hydrogeomorphic floodplain mapping: Insights into human-induced floodplain disconnectivity. *River Res Applic*. 2018;34:675–685. https://doi.org/10.1002/rra.3296